Photophysical poperties of Schiff-base metal complexes

Pier Giorgio Cozzi,* Luisa Stella Dolci, Andrea Garelli, Marco Montalti, Luca Prodi* and Nelsi Zaccheroni

Dipartimento di Chimica "G. Ciamician", Università degli Studi di Bologna, Via Selmi 2, 40126, Bologna, Italy. E-mail: pgcozzi@ciam.unibo.it and lprodi@ciam.unibo.it; Fax: ++39 051 209 9456.

Received (in Montpellier, France) 23rd September 2002, Accepted 18th December 2002
First published as an Advance Article on the web 5th March 2003

The photophysical behaviour of Schiff-base complexes with several different metals has been investigated. Among these complexes, the one with aluminium (**3**) presents interesting features, showing good chemical stability, high absorption coefficients and fluorescence quantum yield. In addition, the fluorescence intensity of **3** udergoes appreciable changes in the presence of coordinating species, such as carboxylate anions, allowing the association process to be monitored with high sensitivity. In addition, we have demonstrated that, if suitable groups are attached to the carboxylate function, supramolecular systems with interesting properties can be designed and characterised.

Introduction

In the last decade Schiff-base ligands have received more and more attention, mainly because of their wide application in the fields of synthesis and catalysis. This attention is still growing, so that a considerable research effort is today devoted to the synthesis of new Schiff-base complexes with transition[1] and main group[2] metal ions, to further develop applications in both catalysis and material chemistry.[3–7] The salen ligand has also been used to activate redox chemistry for the selective recognition and modification of nucleic acids. Adducts formed between guanine and nickel complexes based on salen ligands strongly inhibit polynucleotide elongation, allowing sensitive detection through polymer extension assays.[8–10]

In spite of the great attention devoted to this class of compounds, however, a systematic discussion of the photophysical properties of Schiff-base complexes is still absent in the literature. As a matter of fact, this absence certainly cannot be due to the lack of interesting photophysical features shown by these complexes; in fact, very recently, two Schiff-base aluminium complexes have been, for example, proposed as luminescent biolabels thanks to their high fluorescence intensity.[11] Photoluminescence spectroscopy can indeed help to find solutions to many analytical problems in applications such as medical diagnostics, cell biology and environmental sciences, giving also the possibility to monitor analyte concentrations in real-time and real-space if suitable, highly luminescent probes are used.[12–14] In addition, among the different techniques used to monitor molecular recognition processes, photoluminescence spectroscopy certainly offers great advantages in terms of sensitivity and versatility.[15] As a consequence, this technique could also be used to monitor some of the events occurring in the catalytic processes in which Schiff-base complexes play a so-important role,[16] since the nature of the coordination sphere could be monitored by changes in the luminescence properties.

In this context, a special role can be played, in our opinion, by aluminium salen complexes, which have found interesting applications in catalysis and synthesis. Five-coordinated complexes of aluminium were prepared and described.[17] Cationic complexes are able to promote the oligomerisation of propylene oxide[18] while the neutral complexes have been used in living polymerisation of propylene oxide and lactides.[19] Chiral Al(salen) complexes are able to promote the 1,4-addition of nucleophiles to unsaturated substrates, *via* a coordination of the carbonyl to the aluminium centre.[20] Aluminium salen complexes are easily prepared[21] and neither the chloride nor methyl derivatives are moisture-sensitive. Dissolution in water leads to dissociation of the chloride anion from the aluminium centre and the consequent formation of the cationic dihydrate complex. These kinds of complexes are infinitely stable in water. The photoluminescence properties of Al(salen), coupled with its stability in water, make it a strong candidate for biological essays *in vitro* and *in vivo*.[11] We were interested in evaluating the photophysical properties of Al(salen) for possible use in the detection of substrates able to coordinate to the aluminium centre and change the luminescence of the complex.

For these reasons, we report here the photophysical properties of a series of Schiff-base complexes, together with the effects on the photophysical properties of the aluminium complex upon addition of carboxylate anions. The aim of these latter experiments is to show the possible use of some of the Schiff-base complexes in the construction of supramolecular systems with interesting photophysical properties.

Experimental

Chemicals

All the M(salen) metal complexes were obtained from commercially available (*S*,*S*)-*N*,*N*′-bis-(3,5-di-*tert*-butylsalicylidene)-1,2-cyclohexenediamine (salen, **1**).[22] Co(salen) (**2**) and ClAl(salen) (**3**) are commercially available (Strem). Zn(salen) (**4**) was prepared according to ref. 3. (*N*)Mn(salen) (**5**),[23] (*O*)V(salen) (**6**),[24] Sn(salen) (**7**),[25] ClPhSi(salen) (**8**),[26] and Mg(salen) (**9**),[27] were all prepared according to the literature.

1-Pyrenebutyric acid and tetramethylammonium hydroxyde were purchased from Aldrich. Commercially available (Aldrich) NAH was washed with hexane under nitrogen before use.

DOI: 10.1039/b209396k

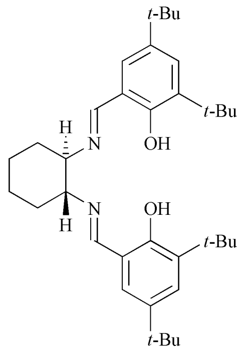

1

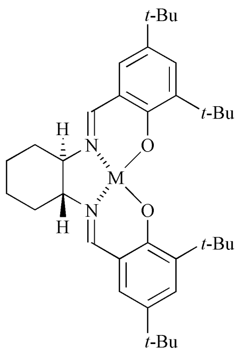

M = Co, **2** ; Zn, **4** ;
Sn, **7** ; Mg, **9**

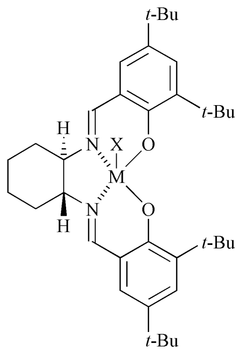

X = Cl, M = Al, **3**
X = N, M = Mn, **5**
X = O, M = V **6**

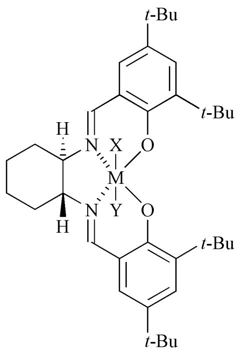

X =Ph, Y = Cl, M = Si, **8**

Spectroscopic measurements

The solvent for photophysical measurements was aerated acetonitrile from Merck (UVASOL) used without further purification. Absorption spectra were recorded with a Perkin Elmer Lambda 40 spectrophotometer. Uncorrected emission and corrected excitation spectra were obtained with a Perkin Elmer LS50 spectrofluorimeter equipped with a Hamamatsu R928 phototube. The fluorescence lifetimes (uncertainty ±5%) were obtained with an Edinburgh single-photon counting apparatus, in which the flash lamp was filled with D_2. Luminescence quantum yields (uncertainty ±15%) were determined using quinine sulfate ($\Phi = 0.546$ in 0.5 M H_2SO_4) as standard.[28] In order to allow comparison of emission intensities, corrections for instrumental response, inner filter effects and phototube sensitivity were performed. A correction for differences in the refraction index was introduced when necessary. Spectrofluorimetric and UV-Vis spectrophotometric titrations were carried out in acetonitrile according to previously published procedures.[29,30]

ESI-MS experiments

HPLC grade acetonitrile and deionised water were used as obtained from Carlo Erba Reagents. Electrospray ionisation mass spectra were obtained with Agilent Technologies MSD1100 single-quadrupole mass spectrometer. Mass spectra were acquired in full-scan mode from m/z 150 to m/z 3000, with a scan time of 0.1 s in the negative ion mode. The parameters of the spray chamber were set as follows: drying gas flow at 10 ml min^{-1}, nebulizer (nitrogen) pressure at 35 psig, temperature at 350 °C, and ESI spray voltage at 5000 V. The fragmentor voltage was maintained at 50 V. All samples are injected in direct mode with an HPLC Agilent Technologies HP1100 equiped with autosampler and were eluted isocratically using a 70:30 mixture of acetonitrile–water.

Results and discussion

Photophysical properties.

The most relevant photophysical properties of the ligand **1** and its metal ion complexes studied in this work are gathered in Table 1. As it can be seen from this table and Fig. 1, the ligand presents two distinct absorption bands in the range 250–400 nm, at 257 and 328 nm. Upon addition of solid NaH (a well-established procedure for deprotonating salen ligands[31,32]), the lower energy band shifts to longer wavelength upon the addition of up to two equivalents of hydride. It is to be noted that all the spectra obtained when less than 2 equiv. of NaH are added are in fact a linear combination of the spectra of the free ligand and the one obtained upon addition of 2 equiv. of NaH. This finding indicates that the mono-deprotonated species is rapidly converted in the bis-deprotonated one. A similar conclusion can be obtained from the fluorescence spectra (Fig. 2): while the ligand is not fluorescent, upon addition of NaH only one band at 436 nm appears, whose corrected intensity[33] is proportional to the amount of hydride added.

Moreover, the excitation spectra ($\lambda_{em} = 436$ nm) are in all cases proportional to the absorption spectrum obtained upon addition of two equivalents of NaH. The shape of this band, the large Stokes shift observed, and its lifetime indicate that the fluorescent excited state is a singlet state, having a geometry considerably distorted compared to that of the ground state.

A large, unstructured band in the 300–400 nm region similar to that observed for the deprotonated form of **1** is also present in the absorption spectra of complexes **3**–**6** and **9** (Table 1 and Figs. 1 and 3). The energy of this band depends on the nature of the metal ion, although it is difficult to make any correlation. The absorption spectra of **7** and **8** (Table 1 and Fig. 3) present in this spectral region only a long, rather weak, tail. In the absorption spectrum of the Co complex **2** (Fig. 1) it is instead present as an additional band. This band, which cannot be attributed to a metal-centred transition (the molar absorbivity is too high), can be assigned with good confidence to a charge transfer transition involving the redox-active metal ion.

Table 1 Photophysical properties of the ligand and its metal complexes in acetonitrile solutions at room temperature

	Absorption		Emission		
Compound	λ_{max}/nm	ε/M^{-1}cm^{-1}	λ_{max}/nm	τ/ns	Φ
1	328	7200	–[a]	–	–
	257	32 000			
1H_{-2}^{2-}	351	13 000	436	6.6	0.08
	257(s)	25 000			
2	411	5500	–[a]	–	–
	353	5750			
	260	27 300			
3	355	9300	476	6.6	0.18
	279	24 000			
4	392	12650	464	5.8	0.14
	276	22 500			
5	385	4600	–[a]	–	–
	247	21 700			
6	373	6800	–[a]	–	–
7	363	4400	495	2.0	0.005
	331	5150			
	235	25 000			
8	343(s)	2420	531	2.1	0.008
	303	14 300			
9	361	10 000	458	6.3	0.19
	240	42 000			

[a] Not luminescent

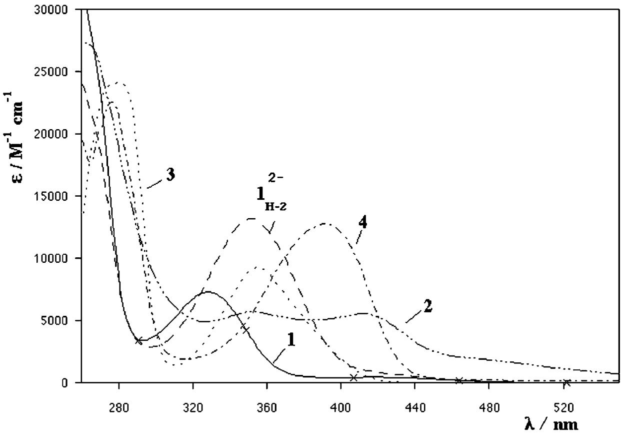

Fig. 1 Absorption spectra of the ligand **1**, of its deprotonated form, and of the complexes **2**–**4** in acetonitrile solutions at room temperature.

The complexes **2**, **5**, and **6** did not show any luminescence; this was an expected result, since complexes of these transition metal ions typically possesses low-energy metal-centred states or can give rise to electron transfer processes involving the redox-active metal ion, thus quenching the luminescence coming from intraligand transitions.[34] The complexes with Al (**3**), Zn (**4**), Sn (**7**), Si (**8**), and Mg (**9**) present an unstructured, large fluorescence band in the 400–700 nm region (Fig. 2), with a lifetime in the nanosecond range. As it was discussed for the deprotonated ligand, these transitions could be assigned as originating from singlet ligand-centred excited states, having a geometry considerably distorted compared to that of the ground state. It is interesting to note that the energy of this transition decreases on increasing the formal charge of the central metal. While **7** and **8** show quite weak fluorescence intensities, **3**, **4**, and **9** present remarkably high quantum yields. Unfortunately, the Mg complex is not very stable in non-anhydrous acetonitrile solutions, while the Zn complex tends to form aggregates,[3] leading to precipitation of the complex. For these reasons, these latter complexes do not seem very promising for use as luminophores in the design of new luminescent chemosensors and labels. On the contrary, the ClAl(salen) complex **3** is stable for days in acetonitrile solutions and, because of its interesting photophysical properties, deserves attention as a possible component of supramolecular structures.

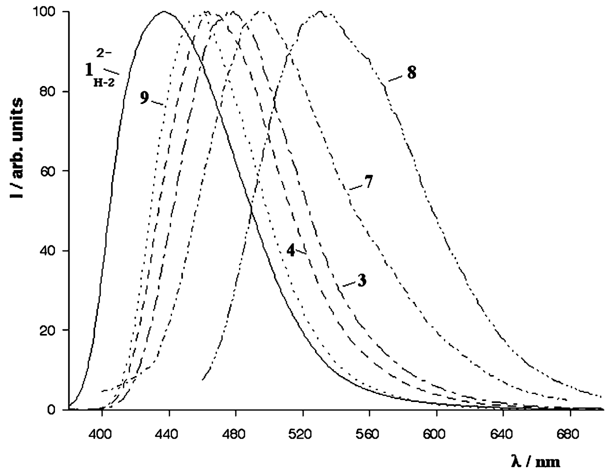

Fig. 2 Fluorescence spectra of the deprotonated form of ligand **1** and of the complexes **3**, **4**, **7**, **8**, and **9** in acetonitrile solutions at room temperature.

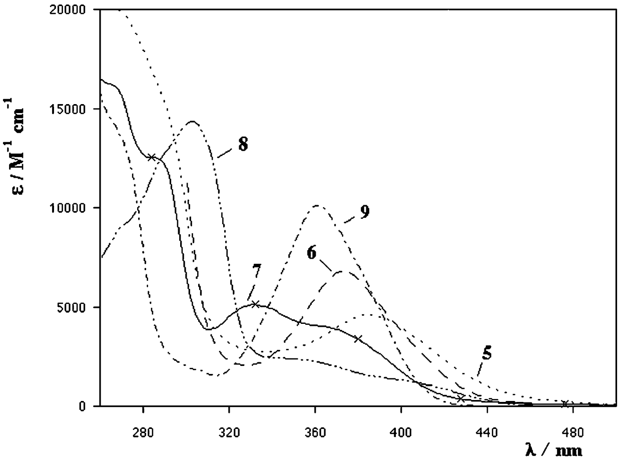

Fig. 3 Absorption spectra of the complexes **5**–**9** in acetonitrile solutions at room temperature.

Adducts between the Al complex and carboxylate anions

In the view of integrating the Al(salen) complex in supramolecular systems, and considering the high affinity usually shown by the hard aluminium centre for carboxylate anions, we added an increasing amount of tetrabutylammonium acetate to an acetonitrile solution of **3**. While the changes observed in the absorption spectrum were almost negligible, noticeable changes could be monitored in the fluorescence intensity. As it can be seen in Fig. 4, the intensity increases, reaching a maximum upon the addition of 0.5 equiv. of acetate anion (Ac^-), while decreasing afterwards before reaching a plateau once 1 equiv. of the salt has been added.

A parallel change of the excited state lifetime can be observed: a longer component (10.4 ns) shows up in the first part of the titration experiment, while a shorter one (4.2 ns) appears after the addition of more than 0.5 equiv. of acetate. This latter component is the only one present at the end of the titration experiments. These findings clearly indicate that two species with different stoichiometries are formed during the titration experiment, one ($\mathbf{3}_2$Ac) in which an acetate anion acts as bridging ligand between two salen complexes and one with a 1:1 stoichiometry, according to the following equilibria:

$$2\mathbf{3} + \mathrm{Ac}^- \leftrightarrow \mathbf{3}_2\cdot\mathrm{Ac} \qquad (1)$$

$$\mathbf{3} + \mathrm{Ac}^- \leftrightarrow \mathbf{3}\cdot\mathrm{Ac} \qquad (2)$$

Interpolation of absorption and fluorescence titration profiles with the global analysis package SPECFIT[35,36] confirmed this qualitative interpretation, allowing us to calculate the

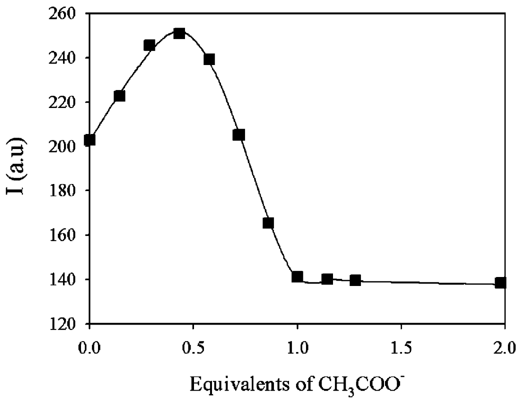

Fig. 4 Fluorescence intensity of an acetonitrile solution of **3** upon addition of increasing amounts of tetrabutylammonium acetate.

constants relative to the two equilibria [logβ_{21} = 14.3 ± 0.3 for eqn. (1) and logβ_{11} = 9.1 ± 0.3 for eqn. (2)]. The formation of the $\mathbf{3}_2$·Ac species was confirmed by ESI-MS measurements, since in the presence of **3** (5×10^{-4} M) and 0.4 equiv. of acetate anion, the signal of the molecular ion $[2M - H + Ac]^-$ at *m*/*z* 1272 was clearly evident. This signal is completely absent when solutions of the ligand alone or upon addition of 1.2 equiv. of acetate are analysed.

As far as the fluorescence band shape is concerned, these two species are both blue-shifted, compared to the complex alone, by 10 nm, indicating that the charge density changes caused by the anion complexation has non-negligible effects on the photophysical properties of the complex. While these changes could be insufficiently large to be used in the design of a sensor device for the acetate anion to use in practical applications, they are large enough to allow the possibility to monitor the association process with high sensitivity.

In order to see whether it was possible, using the Al(salen) platform, to assemble supramolecular systems in which photoinduced processes could occur among the different components, we used as a coordinating ligand the 1-pyrenebutanoate anion (**10**), obtained by neutralising 1-pyrenebutyrric acid with 1 equiv. of tetrabuthylammonium hydroxide. Upon addition of **10** to an acetonitrile solution of **3**, it was possible to observe an increase of the absorbance due to the increased concentration of the pyrene chromophore.[37] Negligible changes were detected in the absorption of the salen complex, similarly to what was observed on adding the acetate anion. As in that case, much larger changes were observed in the fluorescence spectrum. If excitation is performed at 360 nm, a wavelength that is predominantly ($>95\%$) absorbed by the Al complex, upon addition of the carboxylate anion the fluorescence band of **3** undergoes a 10 nm blue-shift. As far as the intensity is concerned, small changes could be detected in the first part of the titration experiment (Fig. 5), while a noticeable quenching occurred afterwards to about 65% of the initial value upon addition of 1 equiv. of **10**. A parallel decrease (to 3.4 ns) of the excited state lifetime was also observed.

As it was found for the acetate anion, interpolation of the fluorescence (λ_{exc} = 360 nm) titration profile showed the presence of two different equilibria, with association constants (logβ_{21} = 13.9 ± 0.3 and logβ_{11} = 8.7 ± 0.3) slightly smaller than those found for the acetate. This was an expected result, because of the larger steric hindrance present in this case. The molar fraction distribution of all the species in solution is shown in Fig. 6. The calculated fluorescence spectra upon excitation at 360 nm shows that the intermediate species $\mathbf{3}_2$·**10** has the highest quantum yield, while the **3**·**10** species showed the lowest one, as it was found in the case of the acetate anion.

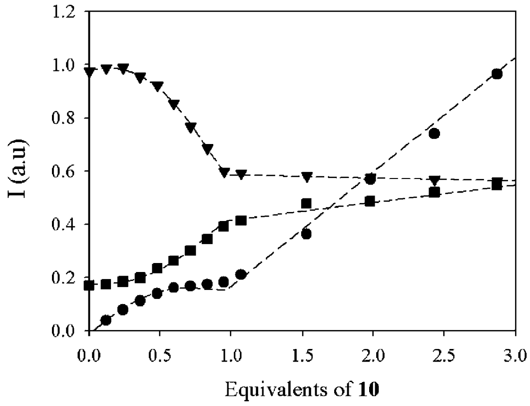

Fig. 5 Fluorescence intensity of an acetonitrile solution of **3** upon addition of increasing amounts of **10** (▼ λ_{exc} = 360 nm, λ_{em} = 480 nm; ● λ_{exc} = 325 nm, λ_{em} = 378 nm; ■ λ_{exc} = 325 nm, λ_{em} = 480 nm).

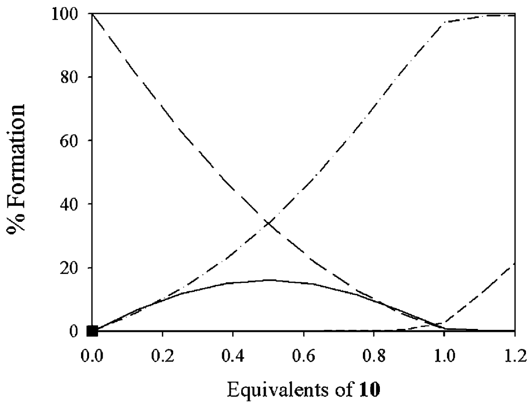

Fig. 6 Molar fraction distribution of the species formed during the titration of **3** with**10**: **3** (— — —), **10** (---), $\mathbf{3}_2$·**10**(——), and **3**·**10**(–·–).

The most interesting results were indeed observed when exciting at 325 nm, where the absorption coefficient of the pyrene is much higher than that of **3**. In this case, two different signals can be monitored, namely the structured fluorescence attributable to the pyrene chromophore, with λ_{max} at 378 nm, and the unstructured band centred on the salen structure, with λ_{max} at 476 nm. In particular, the corrected fluorescence of the pyrene chromophore, although its concentration increases linearly during the titration experiment, showed an increase up to the addition of 0.5 equiv. of the salt, a plateau until 1 equiv. is added, while it steeply increases afterward (Fig. 5). On the contrary, the corrected intensity of the salen complex remains quite low until 0.5 equiv. of **10** is added, while it increases afterwards up to the addition of 1 equiv. of the carboxylate anion; at this point a plateau is reached. These results clearly indicate that in the **3**·**10** adduct, an efficient energy transfer occurs from the pyrene moiety, whose fluorescence is almost completely quenched, to the salen complex inside the supramolecular structure (Scheme 1).

The increase of the fluorescence intensity of the latter moiety, observed in spite of the decrease of its quantum yield discussed above, is due to an increase in the number of photons absorbed by the system that, *via* the energy transfer process, populate the fluorescent excited state. The occurrence of the energy transfer process in **3**·**10** finds further support in the appearance in the excitation spectrum, obtained at λ_{em} = 480 nm (*i.e.* looking at the fluorescence of **3**), of the structured absorption band typical of the pyrene chromophore when this adduct is present. On the contrary, the energy transfer process among the two chromophoric units is almost negligible in the $\mathbf{3}_2$·**10** adduct [Scheme 1(a)]. In the first part of the titration experiment, when less than 0.3 equiv. of **10** are added, the fluorescence of the pyrene unit is not quenched and, at the same time, its absorption bands are absent in the excitation spectra obtained at λ_{em} = 480 nm.

Interpolation of the fluorescence titration profiles obtained at λ_{exc} = 325 nm confirmed this qualitative interpretation, allowing us to calculate the fluorescence spectra of **3**, $\mathbf{3}_2$·**10**, and **3**·**10** upon excitation at this wavelength (Fig. 7). As it can be seen, the fluorescence spectrum of $\mathbf{3}_2$·**10**, in which the energy transfer process is not active, is dominated by the fluorescence band of the pyrene, while the spectrum of **3**·**10** is dominated by the typical fluorescence of the salen complex, as expected when energy is transferred from the pyrene to this latter unit. The most likely reason why the energy transfer process is not efficient in $\mathbf{3}_2$·**10** while it is efficient in **3**·**10** lies in the different geometry of the pyrene chromophore and **3** in the two different complexes. As a matter of fact, the rate of the energy transfer process according to the Förster mechanism[38] depends on the overlap among the fluorescence band of the pyrene and the absorption band of the Al complex,

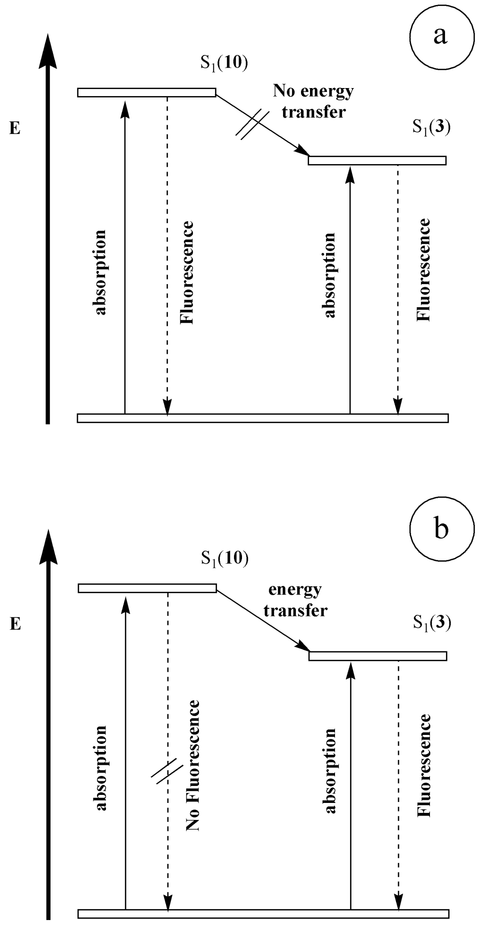

Scheme 1 Schematic energy level diagram of the **3**$_2$·**10** (a) and **3**·**10** (b) adducts and the photophysical process involved.

which do not change substantially on going from **3**$_2$·**10** to **3**·**10**, and on the distance and mutual orientation of the different chromophores, which on the contrary are expected to change upon changing the complex. These two parameters are also very important in determining the electronic coupling that governs the rate according to the Dexter mechanism.[39]

Conclusions

We have presented here the photophysical properties of a large family of salen complexes, which nowadays find widespread use in catalysis and material chemistry. Five of the eight complexes reported in this work show a large, untructured fluorescence band, originating from singlet ligand-centred excited states, having a geometry considerably distorted compared to that of the ground state. Among these complexes, **3** shows the most interesting properties, since it exhibits good chemical stability and has a quite large fluorescence quantum yield. In addition, the fluorescence properties can be changed in the presence of coordinating species such as carboxylate anions and, if suitable groups are attached to the anchoring function, supramolecular systems with interesting properties can be designed and characterised. In particular, if the 1-pyrenebutanoate anion is used, a very efficient energy transfer process can occur from the pyrene unit to the salen complex in the 1:1 **3**·**10** complex. Interestingly, this process is not efficient in the **3**$_2$·**10** complex.

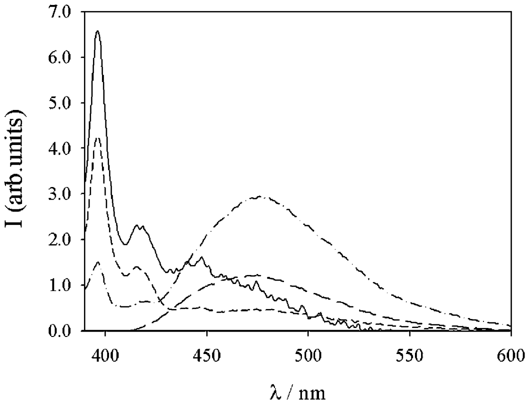

Fig. 7 Calculated fluorescence spectra (λ_{exc} = 325 nm) of the species formed during the titration of **3** with **10**: **3** (— — —), **10** (---), **3**$_2$·**10** (——), and **3**·**10** (—·—).

Acknowledgements

This work was supported by Ministero dell'Università e della Ricerca Scientifica e Tecnologica (MURST, Solid Supermolecules Project) and by the University of Bologna (Funds for Selected Research Topics)

References

1 W. H. Leung, E. Y. Y. Chan, E. K. F. Chow, I. D. Williams and S. M. Peng, *J. Chem. Soc., Dalton Trans.*, 1996, 1229.
2 D. A. Atwood and M. J. Harvey, *Chem. Rev.*, 2001, **101**, 37.
3 G. A. Morris, H. Zhou, C. L. Stern and S. T. Nguyen, *Inorg. Chem.*, 2001, **40**, 3222.
4 M. Bandini, P. G. Cozzi and A. Umani-Ronchi, *Chem. Commun.*, 2002, 919 and references therein.
5 L. Canali and D. C. Sherrington, *Chem. Soc. Rev.*, 1999, **28**, 85.
6 N. Y. Ito and T. Katsuki, *Bull. Chem. Soc. Jpn.*, 1999, **72**, 603.
7 T. Katsuki, *Curr. Org. Chem.*, 2001, **5**, 663.
8 J. G. Muller, L. A. Kaiser, S. J. Paikoff, V. Duarte, N. Tang, R. J. Perez, S. E. Rokita and C. J. Burrows, *Coord. Chem. Rev.*, 1999, **185–186**, 761.
9 X. Zhou, J. Shearer and S. E. Rokita, *J. Am. Chem. Soc.*, 2000, **122**, 9046.
10 N. Tang, J. G. Muller, C. J. Burrows and S. E. Rokita, *Biochemistry*, 1999, **38**, 16 648.
11 M. S. J. Briggs, J. S. Fossey, C. J. Richards, B. Scott and J. Whateley, *Tetrahedron Lett.*, 2002, **43**, 5169.
12 (*a*) A. P. de Silva, H. Q. N. Gunaratne, T. Gunnlaugsson, A. J. M. Huxley, C. P. McCoy, J. T. Rademacher and T. E. Rice, *Chem. Rev.*, 1997, **97**, 1515; (*b*) L. Fabbrizzi, M. Licchelli and P. Pallavicini, *Acc. Chem. Res.*, 1999, **32**, 846.
13 (*a*) L. Prodi, F. Bolletta, M. Montalti and N. Zaccheroni, *Coord. Chem. Rev.*, 2000, **205**, 59; (*b*) C. Bargossi, M. C. Fiorini, M. Montalti, L. Prodi and N. Zaccheroni, *Coord. Chem. Rev.*, 2000, **208**, 17.
14 (*a*) L. Prodi, C. Bargossi, M. Montalti, N. Zaccheroni, N. Su, J. S. Bradshaw, R. M. Izatt and P. B. Savage, *J. Am. Chem. Soc.*, 2000, **122**, 6769; (*b*) G.-P. Xue, J. S. Bradshaw, N. K. Dalley, P. B. Savage, K. E. Krakowiak, R. M. Izatt, L. Prodi, M. Montalti and N. Zaccheroni, *Tetrahedron*, 2001, **57**, 7623; (*c*) G. Xue, J. S. Bradshaw, N. K. Dalley, P. B. Savage, R. M. Izatt, L. Prodi, M. Montalti and N. Zaccheroni, *Tetrahedron*, 2002, **58**, 4809; (*d*) L. Prodi, M. Montalti, N. Zaccheroni, G. Pickaert, L. Charbonnière and R. Ziessel, *New J. Chem.*, 2003, **27**, 134.
15 (*a*) M. Montalti and L. Prodi, *Chem. Commun.*, 1998, 1461; (*b*) L. La Monica, D. Monti, G. Mancini, M. Montalti, L. Prodi, N. Zaccheroni, R. Paolesse and G. D'Arcangelo, *New J. Chem.*, 2001, **25**, 597.
16 M.-A. Munoz-Hernandez, M. L. McKee, T. S. Keizer, B. C. Yearwood and D. A. Atwood, *J. Chem. Soc., Dalton Trans.*, 2002, 410.
17 M.-A. Munoz-Fernandez, T. S. Keizer, P. Wei, S. Parkin and D. A. Atwood, *Inorg. Chem.*, 2001, **40**, 6782.
18 W. Braune and J. Okuda, *Angew. Chem., Int. Ed.*, 2003, **42**, 64.
19 R. M. Ovitt and G. W. Coates, *J. Am. Chem. Soc.*, 1999, **121**, 4072.
20 J. K. Myers and E. N. Jacobsen, *J. Am. Chem. Soc.*, 1999, **121**, 8959.

21 D. A. Atwood, J. A. Jegier and D. Rutheford, *Inorg. Chem.*, 1996, **35**, 63.

22 For the structure of the ligand see: D. J. Darensbourg and J. C. Yarbrough, *J. Am. Chem. Soc.*, 2002, **124**, 6355.

23 (*a*) J. Du Bois, C. S. Tomooka, J. Hong, E. M. Carreira and M. W. Day, *Angew. Chem., Int. Ed. Engl.*, 1997, **36**, 1645; (*b*) C. J. Chang, W. B. Connick, D. W. Low, M. W. Day and H. B. Gray, *Inorg. Chem.*, 1998, **37**, 3107.

24 S. Bunce, R. J. Cross, L. J. Farrugia, S. Kunchandy, L. L. Meason, K. W. Muir, M. O'Donnel, R. D. Peacock, D. Stirling and S. J. Teat, *Polyhedron*, 1998, **17**, 4179.

25 A. M. Van den Bergen, J. D. Cashion, G. D. Fallon and B. O. West, *Aust. J. Chem.*, 1990, **43**, 1559.

26 J. Wagler, U. Böhme and G. Roewer, *Angew. Chem., Int. Ed.*, 2002, **41**, 1732.

27 Mg(salen) was prepared by addition of *n*-Bu_2Mg to a solution of salen in THF. The Lewis acid catalytic properties of Mg(salen) are under active investigation.

28 S. R. Meech and D. Phillips, *J. Photochem.*, 1983, **23**, 193.

29 M. Montalti, L. Prodi, N. Zaccheroni, L. J. Charbonnière, L. Douce and R. Ziessel, *J. Am. Chem. Soc.*, 2001, **123**, 12 694.

30 L. J. Charbonnière, R. Ziessel, M. Montalti, L. Prodi, N. Zaccheroni, C. Boehme and G. Wipff, *J. Am. Chem. Soc.*, 2002, **124**, 7779.

31 M. Mazzanti, J.-M. Rosset, C. Floriani, A. Chiesi-Villa and C. Guastini, *J. Chem. Soc., Dalton Trans.*, 1989, 953.

32 E. Solari, C. Maltese, F. Franceschi, C. Floriani, A. Chiesi-Villa and C. Rizzoli, *J. Chem. Soc., Dalton Trans.*, 1997, 2903.

33 A. Credi and L. Prodi, *Spectrochim. Acta, Part A*, 1998, **54**, 159.

34 (*a*) L. Fabbrizzi, M. Licchelli, P. Pallavicini, A. Perrotti, A. Tagletti and D. Sacchi, *Chem.-Eur. J.*, 1996, **2**, 75; (*b*) L. Prodi, M. Montalti, N. Zaccheroni, F. Dallavalle, G. Folesani, M. Lanfranchi, R. Corradini, S. Pagiari and R. Marchelli, *Helv. Chim. Acta*, 2001, **84**, 690.

35 SPECFIT: R. A. Binstead, Spectrum Software Associates, Chapel Hill, NC, 1996.

36 M. Montalti, L. Prodi, N. Zaccheroni and G. Falini, *J. Am. Chem. Soc.*, 2002, **124**, 13 540.

37 A. Juris and L. Prodi, *New J. Chem.*, 2001, **25**, 1132.

38 T. Förster, *Discuss. Faraday Soc.*, 1959, **27**, 7.

39 D. L. Dexter, *J. Chem. Phys.*, 1953, **21**, 836.